LRP 720/02 February 2002

Thermodynamic Optimisation of 70 kA Binary Current Lead (Final Report)

R. Wesche

CRPP
Centre de Recherches en Physique des Plasmas
Association Euratom - Confédération Suisse

ÉCOLE POLYTECHNIQUE
FÉDÉRALE DE LAUSANNE

Centre de Recherches en Physique des Plasmas (CRPP)
Association Euratom - Confédération Suisse
Ecole Polytechnique Fédérale de Lausanne
PPB, CH-1015 Lausanne, Switzerland
phone: +41 21 693 34 82 / 87 — fax +41 21 693 51 76

Centre de Recherches en Physique des Plasmas
Technologie de la Fusion (CRPP-TF)
Association Euratom - Confédération Suisse
Ecole Polytechnique Fédérale de Lausanne
CH-5232 Villigen-PSI, Switzerland
phone: +41 56 310 32 59 — fax +41 56 310 37 29

http://crppwww.epfl.ch/

LRP 720/02 February 2002

Thermodynamic Optimisation of 70 kA Binary Current Lead (Final Report)

R. Wesche

ISSN 0458-5895

ÉCOLE POLYTECHNIQUE
FÉDÉRALE DE LAUSANNE

LRP 720/02 **February 2002**

Thermodynamic Optimisation of 70 kA Binary Current Lead

Final Report

R. Wesche

École Polytechnique Fédérale de Lausanne
Centre de Recherches en Physique des Plasmas – Fusion Technology
c/o Paul Scherrer Institute
WMHA/C31
CH-5232 Villigen PSI
Switzerland

Introduction

In the frame of the European Fusion Technology Programme, the Forschungszentrum Karlsruhe (FZK) and the Centre de Recherches en Physique des Plasmas (CRPP) are developing a 70 kA current lead for the toroidal field coil system of the International Thermonuclear Experimental Reactor ITER-FEAT using high-temperature superconductors (HTS). In the first phase of this program two 10 kA current leads based on Ag/Au stabilised Bi-2223 tapes have been already successfully tested at CRPP [1,2]. These binary current leads consist of a conduction-cooled HTS and a wire bundle type heat exchanger part actively cooled by 60 K helium gas.

Metallic current leads required to connect the superconducting magnets with the power supplies located at room temperature introduce heat due to Joule heating and heat conduction. A minimum heat leak of 1.04 W/kA results for an optimised gas-cooled conventional current lead for ideal heat transfer [3]. Commercial current leads operating between 4.5 and 293 K cause a heat leak of ≈1.16 W/kA [4]. The power required to cool the conventional metallic current leads of a superconducting magnet operated at 4.5 K is therefore a substantial fraction of the total electric input power consumed by the refrigerator. Using superconducting current leads Joule heating can be eliminated in the temperature range of 4.5 – ≈70 K which provides the possibility to reduce the heat load at 4.5 K by a factor of 10. However, comparing superconducting and conventional current leads, it is the electric input power of the refrigerator required to cool the whole current lead rather than the heat load at 4.5 K which has to be considered. Due to the considerably enhanced refrigerator efficiency for a helium inlet temperature of 60 K savings of 60 – 80 % can be achieved in the electrical input power required to cool the current leads [5].

Presently, the inlet temperature of the helium gas required to cool the copper part of the current leads of the toroidal field coils has not been fixed in the ITER-FEAT design. Furthermore, studies performed at CERN indicate that the optimum temperature at the warm end of the superconductor of the 13 kA current leads for the Large Hadron Collider (LHC) is 50 K for a helium inlet temperature of 20 K [6]. Consequently, the effect of both the helium inlet temperature and the warm end temperature of the superconductor on the performance of the 70 kA current leads for the toroidal field coils of ITER-FEAT has to be studied within the present development program.

Numerical Simulation

In this section the numerical simulation of gas-cooled current leads is described. The numerical method is illustrated in Fig. 1. In the case of finite heat transfer the temperature profile along the current lead is described by the following two differential equations

$$\frac{d}{dx}\left[\lambda(T)\frac{dT}{dx}\right]+\frac{\rho(T)I^2}{A^2}-\frac{hP}{A}(T-\theta)=0 \tag{1}$$

$$hP(T-\theta)=\dot{m}c_p\frac{d\theta}{dx} \tag{2}$$

where x is the distance from the cold end, T the conductor temperature, λ the thermal conductivity, ρ the electrical resistivity, A the conductor cross-section, I the current, θ the gas temperature, h the heat transfer coefficient, P the cooled perimeter, c_p the gas specific heat and

$\dot{m}$ the mass flow rate. For the numerical simulation the current lead has to be divided into many short segments. Neglecting the temperature dependence of the properties of the materials and the variation of $\Delta T = T - \theta$ within one segment, equation (1) can be approximately solved and we obtain

$$T(x) = -\frac{a}{2}x^2 + bx + c \tag{3}$$

where

$$a = \frac{\rho I^2}{\lambda A^2} - \frac{hP}{\lambda A}\Delta T \tag{4}$$

The integration constants b and c can be determined using the boundary conditions at the cold end of the segment. The approximate solution for $T(x)$ is used to calculate $T(\Delta x)$ and $\dot{Q}(\Delta x)$ at the warm end of the segment. The change of the gas temperature is given approximately by

$$\Delta\theta = \frac{hP\Delta T}{\dot{m}c_p}\Delta x \tag{5}$$

where Δx is the length of a single segment.

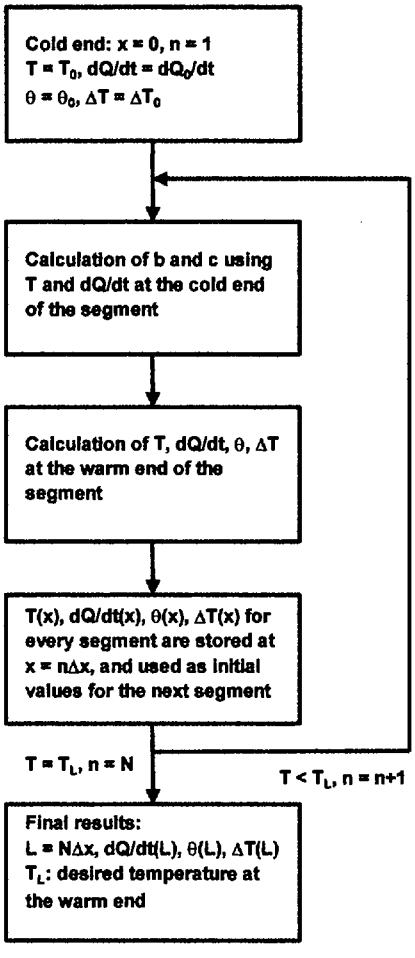

Fig. 1. Illustration of numerical method for simulating gas-cooled current leads (after [5]).

Using $\Delta\theta$ the temperature difference of coolant and conductor at the warm end of the segment is calculated. $T(\Delta x)$, $\dot{Q}(\Delta x)$ and $\Delta T(\Delta x)$ are used as the initial values for the next step of the simulation. The procedure is repeated until the desired temperature T_L at the warm end of the current lead is reached.

Superconducting Part of the Current Lead

In the present calculations the power generated in the interconnection of the superconducting and the copper part of the binary current lead is neglected. At the joint of the superconducting and the copper part continuity of the heat flux has been taken into consideration. Thus, the heat flux at the cold end of the heat exchanger is equal to the heat load at the cold end of the high-T_c superconductor. The heat leak at the cold end of a AgAu/Bi-2223 current lead without a stainless steel support is

$$\dot{Q}_0 = \frac{A_{AgAu}}{L_{sc}} \int_{4.5K}^{T_i} \lambda_{AgAu}(T)dT \tag{6}$$

where L_{sc} is the length of the superconductor, T_i the temperature at the warm end of the superconductor and $A_{AgAu} = f_{AgAu}A_{AgAu/Bi\text{-}2223}$. The contribution of the Bi-2223 superconductor to heat conduction is negligible because of the extremely small thermal conductivity of this material, which is more than one order of magnitude smaller than that of the AgAu matrix. Furthermore, the fraction f_{AgAu} of the AgAu matrix in the conductor cross-section is as large as 70 %. In the model calculations it has been assumed that the design value of the critical current is 95.5 kA at the desired temperature T_i at the warm end of the superconductor. The resulting cross-section of the AgAu matrix is

$$A_{AgAu} = f_{AgAu}\frac{95.5kA}{j_e(B,T)} \tag{7}$$

where $j_e(B,T)$ is the engineering critical current density with respect to the total conductor cross-section including the AgAu matrix.

In reality the stacks of superconducting AgAu/Bi-2223 tapes need to be mechanically supported by a stainless steel tube. The heat capacity of the superconducting current lead is considerably enhanced by the additional stainless steel. Due to the larger heat capacity a prolonged time is available before the critical temperature of the superconductor is reached in the case of loss of flow in the heat exchanger part of the current lead. In principle, the same effect can be reached by an enlarged superconductor cross-section. However, additional superconductor is more expensive than stainless steel and would lead to a more pronounced increase of the heat leak at 4.5 K. The reason for this behaviour is the fact that the thermal conductivity of AgAu is larger than that of stainless steel. Consequently, an overdimensioned stainless steel support may be used to reach the ITER-FEAT safety requirements.

In the HTS part of the current lead the stainless steel support tube and the AgAu/Bi-2223 superconductor are in good thermal contact. To determine the temperature profile along the HTS part of the current lead the thermal conductivities averaged over the total cross-section including the stainless steel support have to be used. The heat load at the cold end is

$$\dot{Q}_0 = \frac{A}{L}\int_{4.5K}^{T_i}\left(f_{steel}\lambda_{steel}(T) + (1 - f_{steel})\lambda_{AgAu}(T)\right)dT \tag{10}$$

where L is the length of the HTS part, $A = A_{AgAu} + A_{steel}$ and $f_{steel} = A_{steel}/A$. Rearrangement of equation (10) leads to

$$\dot{Q}_0 = \frac{A_{steel}}{L}\int_{4.5K}^{T_i}\lambda_{steel}(T)dT + \frac{A_{AgAu}}{L}\int_{4.5K}^{T_i}\lambda_{AgAu}(T)dT \tag{11}$$

Thus, the heat load at the cold end can be calculated considering the superconductor and the stainless steel support separately.

Material Data

In this section the material data used in the simulations are briefly described. For the heat exchanger part copper with residual resistivity ratios of 30 and 50 has been considered. The resistivity and the thermal conductivity data for these two values of the residual resistivity ratio are shown in Figures 2 and 3, respectively.

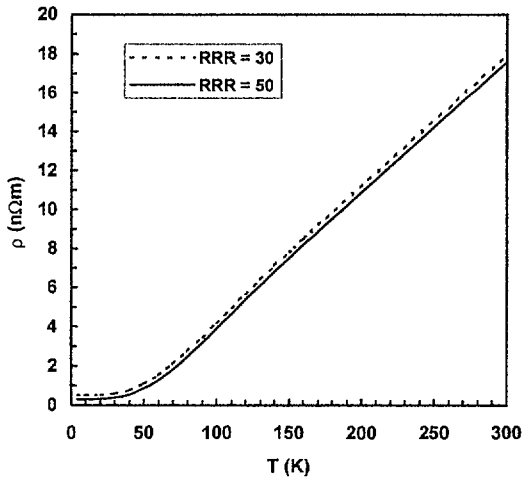

Fig. 2. Resistivity of Cu as a function of temperature for *RRR* values of 30 and 50.

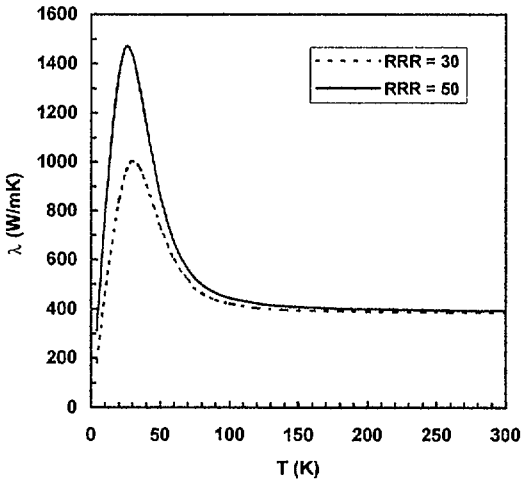

Fig. 3. Thermal conductivity of Cu as a function of temperature for *RRR* values of 30 and 50.

In the outline design of the 70 kA current leads for ITER-FEAT an outer diameter of 160 mm is envisaged for the HTS part of the current lead. The HTS conductor is formed of 20 stacks of AgAu/Bi-2223 tapes. The stack dimensions are 1.8 mm in width and 22.86 mm in thickness. To minimise the magnetic field at the superconductor the stacks are arranged in such a way that a nearly cylindrical conductor would result. The design values of the maximum magnetic fields parallel and perpendicular to the broad face of the single tapes are 157.4 and 68.1 mT, respectively [7]. The engineering critical current density of the AgAu/Bi-2223 tapes reaches 16 kA/cm^2 at 77 K and zero applied field. Fig. 4 shows the engineering critical current densities normalised to the value at 77 K and $B = 0$ for the maximum magnetic fields parallel and perpendicular to the tape surface as a function of temperature. The values have been estimated using a Mathcad program provided by American Superconductor Corporation. The data indicate that the field perpendicular to the tapes limits the critical current of the current lead.

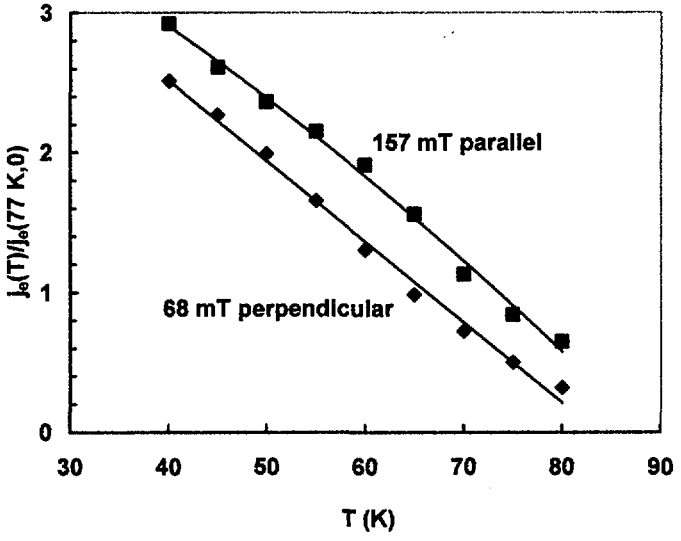

Fig. 4. Estimated engineering critical current densities of the AgAu/Bi-2223 tapes for magnetic fields of 157 mT parallel and 68 mT perpendicular to the tape surface normalised to the j_e value at 77 K and $B = 0$. The current carrying capacity of the current lead is limited by the magnetic field perpendicular to the tape surface.

The expected engineering critical current densities for the unfavourable field direction are used to determine the superconductor cross-section required to reach a critical current of 95 kA. Fig. 5 shows the thermal conductivity of the AgAu matrix as a function of temperature. The data can be fitted by the polynom

$$\lambda_{AgAu} = a_{AgAu}T^4 + b_{AgAu}T^3 + c_{AgAu}T^2 + d_{AgAu}T + e_{AgAu} \tag{12}$$

where the thermal conductivity is expressed in the unit W/mK. The coefficients are listed in Table 1. Values of the integrated thermal conductivity of AgAu for a temperature of 4.5 K at the cold end are listed in Table 2. The data indicate that a reduction of the temperature at the warm end of the superconductor reduces the heat load at 4.5 K considerably due to the reduced integrated thermal conductivity. In addition, the critical current densities increase with decreasing temperature T_i at the warm end (see Fig. 4). On the other hand, the specific heat of the conductor is reduced as a consequence of reduced temperatures and cross-sections, which is undesirable regarding loss of flow in the heat exchanger part of the current lead.

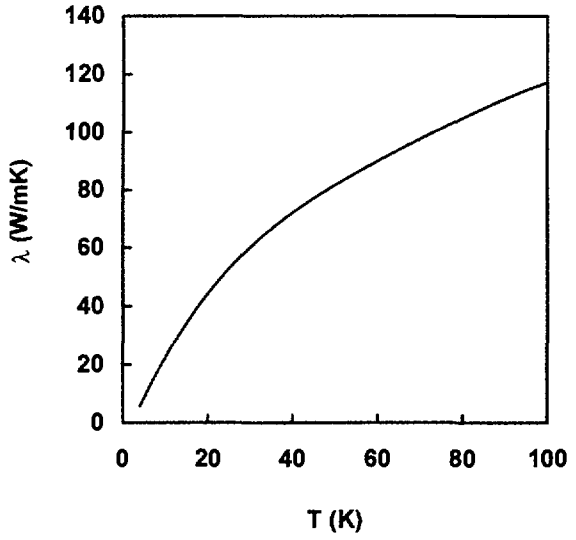

Fig. 5. Thermal conductivity of Ag 3 atom % Au as a function of temperature.

Table 1. Coefficients used to represent the thermal conductivity data of Ag 3 atom % Au.

a_{AgAu}	-1.7465×10^{-6}
b_{AgAu}	4.9848×10^{-4}
c_{AgAu}	-5.4966×10^{-2}
d_{AgAu}	3.5040
e_{AgAu}	-7.4913

Table 2. Values of the integral $Int_{AgAu} = \int_{4.5K}^{T_i} \lambda_{AgAu} dT$.

T_i (K)	Int_{AgAu} (W/m)
40	1614
45	1988
50	2385
55	2804
60	3243
65	3703
70	4181
75	4678
80	5192

Fig. 6 shows the thermal conductivity of stainless steel (ANSI 304). The data can be well represented by the following polynom

$$\lambda_{steel} = a_{steel}T^3 + b_{steel}T^2 + c_{steel}T + d_{steel} \tag{13}$$

where the thermal conductivity is expressed in the unit W/mK. The values of the coefficients are listed in Table 3. Values of the integrated thermal conductivity of stainless steel (ANSI 304) for a temperature of 4.5 K at the cold end are listed in Table 4. Again the integrated thermal conductivity decreases considerably with decreasing temperature at the warm end.

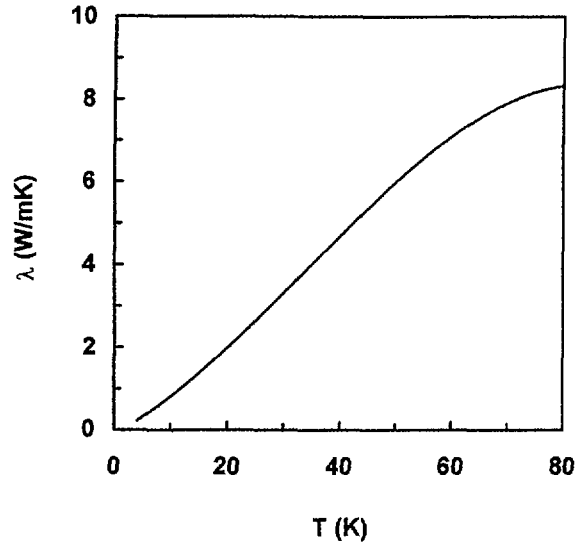

Fig. 6. Thermal conductivity of stainless steel (ANSI 304) as a function of temperature.

Table 3. Coefficients used to represent the thermal conductivity data of stainless steel (ANSI 304).

a_{steel}	-1.8436×10^{-5}
b_{steel}	1.8562×10^{-3}
c_{steel}	7.4769×10^{-2}
d_{steel}	-1.0323×10^{-1}

Table 4. Values of the integral $Int_{steel} = \int_{4.5K}^{T_i} \lambda_{steel} dT$.

T_i (K)	Int_{steel} (W/mK)
40	83
45	108
50	136
55	168
60	202
65	239
70	277
75	317
80	359

Results

First, the steady state performance of the heat exchanger part of the binary current lead is considered. The input values selected for the numerical simulations are summarised in Table 5. The optimum value of the mass flow rate and the length of the current lead is reached when the heat input at the warm end of the heat exchanger is zero, i. e. $dT/dx(L) = 0$. The calculated optimum length which results for a fixed value of the copper cross-section depends strongly on the exact mass flow rate (number of digits taken into consideration). A mass flow rate smaller than the optimum value would result in a maximum of the temperature slightly

below the upper end of the current lead. In the case of loss of flow this temperature maximum would rapidly increase resulting in burn-out of the current lead. Consequently a mass flow rate lower than the optimum value has to be avoided. On the other hand, a mass flow rate which exceeds the optimum value leads to an overcooled current lead, and hence a considerable heat flux enters the current lead at the warm end. Mass flow rates slightly higher than the optimum value can be used to reduce the length of the heat exchanger.

Table 5. Input values selected for the simulations of the heat exchanger part of the 70 kA current lead.

Copper	RRR = 50	RRR = 30
Current density	1.07 kA/cm^2	1.07 kA/cm^2
Copper cross-section	63.6 cm^2	63.6 cm^2
Nominal current	68 kA	68 kA
Specific heat of He	5.21 J/gK	5.21 J/gK
T_{in} (He inlet temperature)	20 – 70 K	20 – 70 K
T_i (cold end of heat exchanger)	45 – 80 K	45 – 80 K
T_{end} (warm end of heat exchanger)	293 K	293 K
$h \times P$	20000 W/mK	40000 W/mK

The numerical simulation is based on the subdivision of the heat exchanger in many short segments. It is therefore of importance to proof that for a sufficiently large number of segments the solutions are independent of the length of the segments. Fig. 7 shows the optimum value of the mass flow rate as a function of the segment length for copper with a residual resistivity ratio of 30, a conductor temperature of 80 K and a heat flux of 0.5 W at the cold end of the heat exchanger. The helium inlet temperature and the product of the heat transfer coefficient and the cooled perimeter are 60 K and 40000 W/mK, respectively. The values of the optimum mass flow rate are practically independent of the segment length for $\Delta x \leq 10^{-5}$ m.

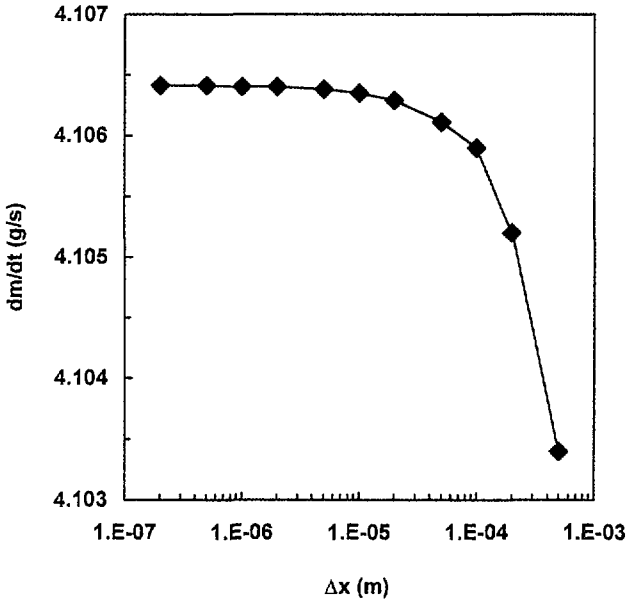

Fig. 7. Optimum mass flow rate versus segment length Δx used in the numerical simulation. The data are for a temperature of 80 K (Cu *RRR* = 30) and a heat flux of 0.5 W at the cold end of the heat exchanger. The He inlet temperature is 60 K and hP = 40000 W/mK.

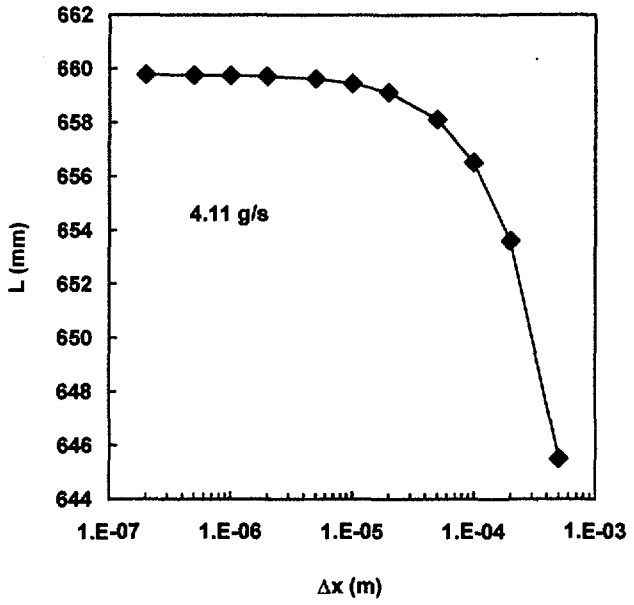

Fig. 8. Length of the heat exchanger versus the segment length Δx used in the numerical simulation. The data are for a temperature of 80 K (Cu *RRR* = 30) and a heat flux of 0.5 W at the cold end of the heat exchanger. The He inlet temperature is 60 K and $hP = 40000$ W/mK.

Fig. 8 shows the length of the heat exchanger as a function of the segment length used in the numerical simulation. The resulting length is practically independent of the segment length for $\Delta x \leq 10^{-5}$ m. Consequently most of the simulations have been done with a segment length of 10^{-6} m.

The temperature profile along the heat exchanger has been calculated with a constant value of *hP* of 20000 or 40000 W/mK. According to the outline design of the binary 70 kA HTS current lead the value of *hP* is between 24000 and 33000 W/mK for temperatures in the range of 70 – 220 K. Fig. 9 shows the dependence of the optimum mass flow rate and the length of the heat exchanger on the value of *hP*. For *hP* values in excess of 10000 W/mK the mass flow rate as well as the length depend only weakly on this parameter. It may be therefore expected that the results are not considerably affected by the use of a constant value of *hP*.

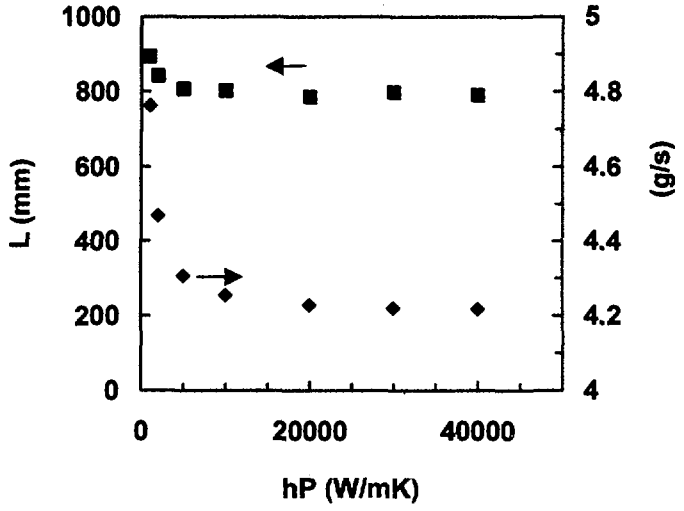

Fig. 9. Optimum mass flow rate and length of the heat exchanger as a function of the value of *hP*. For the calculations $T_{in} = 55$ K, $\Delta T = 15$ K, $RRR = 30$ and $\dot{Q}_0 = 5$ W have been used.

The main goal of the use of binary HTS current leads is the reduction of the electrical input power required by the refrigerator to cool the current leads. The power consumed by a conventional current lead is determined by the heat load at the cold end. Using a binary HTS current lead the heat load at the cold end can be reduced by a factor of 10. However, the power required to cool the heat exchanger part of the current lead has to be taken into consideration. First, let us consider ideal reversible cooling cycles. The input power of the refrigerator required to remove the heat load $\dot{Q}_0$ at 4.5 K is

$$P_{ideal} = \frac{300K - 4.5K}{4.5K}\dot{Q}_0 \tag{14}$$

The prefactor in equation (14) is the inverse of the Carnot efficiency (65.7 W_{el}/W_{th}). To cool the heat exchanger part of the current lead high presssure helium gas provided by the refrigerator in addition to the 4.5 K helium may be used. For example in the SULTAN test facility helium gas of 68 K and a pressure of 16 bar is available to cool the cryogenic shields. Considering again an ideal cooling cycle the power required to cool helium gas from 300 K to a temperature T_{in} is given by the following expression

$$P = \dot{m}\{T_1[s(T_1) - s(T_2)] - [h(T_1) - h(T_2)]\} \tag{15}$$

where s is the entropy and h the enthalpy of the helium gas, T_1 = 300 K and $T_2 = T_{in}$. Fig. 10 shows the work required to cool 1 g of helium gas (p = 16 bar) to a temperature T_{in} as a function of the helium inlet temperature. This minimum work is 2863 J/g and 1075 J/g for helium inlet temperatures of 20 and 70 K, respectively. The minimum work to cool helium gas from 300 K to a temperature T_{in} depends only weakly on the selected pressure. The input power required by the refrigerator to cool the whole current lead is

$$P = \frac{300K - 4.5K}{4.5K}\dot{Q}_0 + \dot{m}\{T_1[s(T_1) - s(T_2)] - [h(T_1) - h(T_2)]\} \tag{16}$$

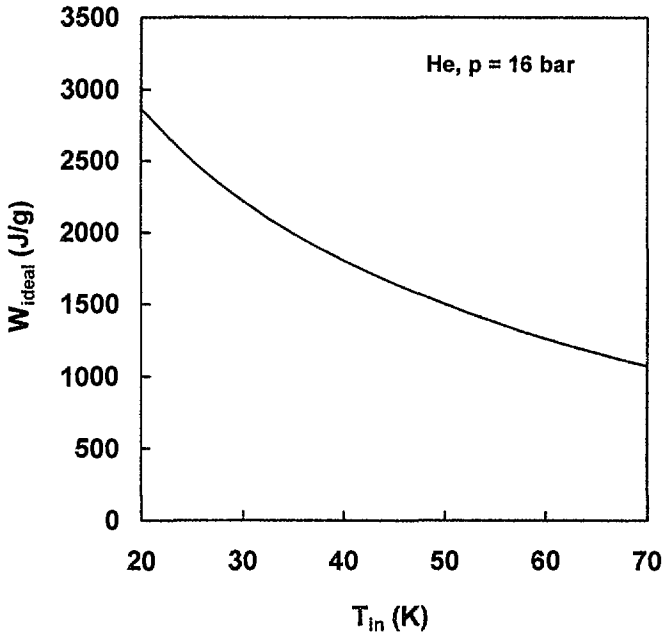

Fig. 10. Minimum work required to cool 1 g helium gas from room temperature to the temperature T_{in}.

The efficiency of a real refrigerator is considerably smaller than the efficiency of an ideal perfectly reversible cooling cycle. The input power required to remove a thermal load of 1 W at 4.5 K is for example between 220 and 700 W. In the case of a large refrigerator 30 % of the ideal efficiency may be reached for helium gas of 60 K inlet temperature. If we assume that the ratio of the real and the ideal efficiency is independent of the operating temperature, the optimum intermediate conductor temperature (warm end of HTS, cold end of heat exchanger) would be the same as for an ideal cooling cycle. However, if the ratio of real and ideal efficiency depends on the helium inlet temperature T_{in} the optimum intermediate conductor and the helium inlet temperature would be different from the values resulting for ideal cooling cycles.

For the heat load at 4.5 K a coefficient of performance of 400 W_{el}/W_{th} has been selected for the model calculations. Furthermore, it is assumed that the efficiency to cool helium gas from room temperature to T_{in} is

$$\frac{\eta_{eff}}{\eta_{ideal}} = 0.6\left(\frac{T_{in}}{300K}\right)^{0.43} \tag{17}$$

Temperature profile along the heat exchanger

Figures 11 and 12 show the temperature profiles along the heat exchanger for two slightly different mass flow rates close to the optimum value. A comparison of the two figures indicates that the resulting optimum length of the heat exchanger depends strongly on small changes in the mass flow rate. As a consequence there results a considerable scatter in the calculated length of the heat exchanger when the optimum mass flow rate is calculated with an accuracy of 0.01 g/s.

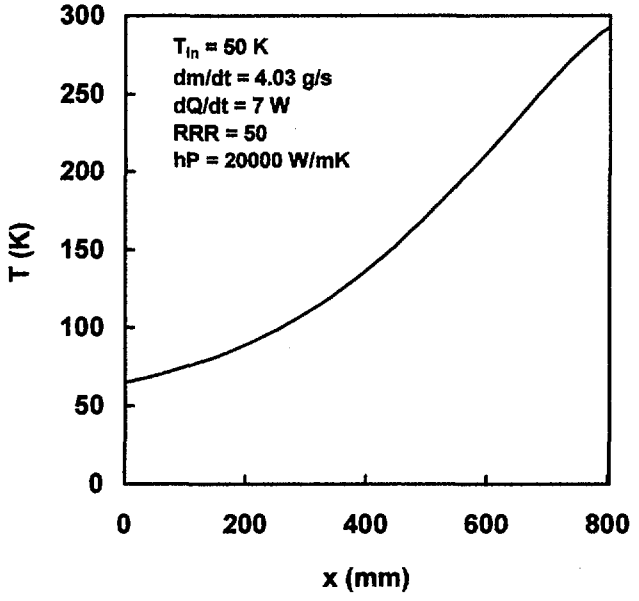

Fig. 11. Temperature profile along the heat exchanger of a binary current lead for a current of 68 kA and a heat flux of 7 W at the cold end. The mass flow rate is slightly higher than the optimum value.

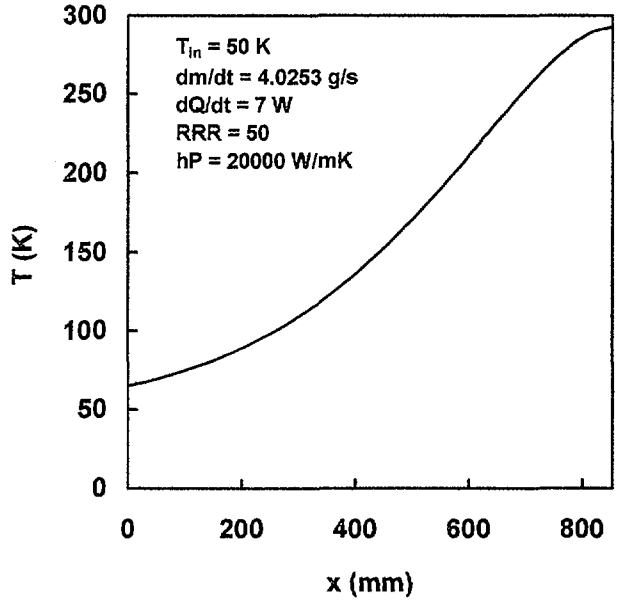

Fig. 12. Temperature profile along the heat exchanger of a binary current lead for a current of 68 kA and a heat flux of 7 W at the cold end. The mass flow rate is slightly lower than that for the results shown in Fig. 11. As a consequence of the reduced mass flow rate the heat input at the warm end is now much closer to zero than in Fig. 11. Moreover, the length of the heat exchanger is enhanced by ≈5 cm.

Binary current lead of 1360 mm length (Cu *RRR* = 50, *hP* = 20000 W/mK, j_e(77 K, 0) = 16 kA/cm^2)

Fig. 13 shows the optimum length of the heat exchanger as a function of the copper temperature at the cold end. The data shown in Fig. 13 are average values for heat fluxes of 0.5, 5, 10, 15, 20, 30 and 40 W at the cold end of the heat exchanger. The observed scatter is a consequence of the sensitivity of the results to the mass flow rate. Generally, the optimum length of the heat exchanger decreases with increasing copper temperature at the cold end. Furthermore, a reduction of the length results for lower helium inlet temperatures.

Fig. 14 shows the heat load at 4.5 K, which results for a design value of the critical current of 95 kA and an engineering critical current density of 16 kA/cm^2 at 77 K and zero applied field. The cross-section of the stainless steel support of the HTS part of the current lead is 40 cm^2. Furthermore, a constant length of the binary current lead of 1360 mm has been selected. In the model calculations the warm and cold end connections as well as the connection between the HTS and the heat exchanger have not been taken into consideration. As long as the heat exchanger part is sufficiently short the heat load at 4.5 K decreases with decreasing temperature at the warm end of the HTS part. Reduced helium inlet temperatures lead to smaller heat loads at 4.5 K. Fig. 15 shows the mass flow rates required to cool the heat exchanger part of the binary current lead for a current of 68 kA. The heat flux at the cold end of the heat exchanger is equal to the heat load at 4.5 K. The length of the heat exchanger part has been varied to minimise the required mass flow rate. In general, the required mass flow rates decrease with increasing temperatures at the cold end of the heat exchanger. Even more pronounced is the effect of the temperature difference of coolant and conductor at the cold end. Larger temperature differences lead to considerably reduced mass flow rates.

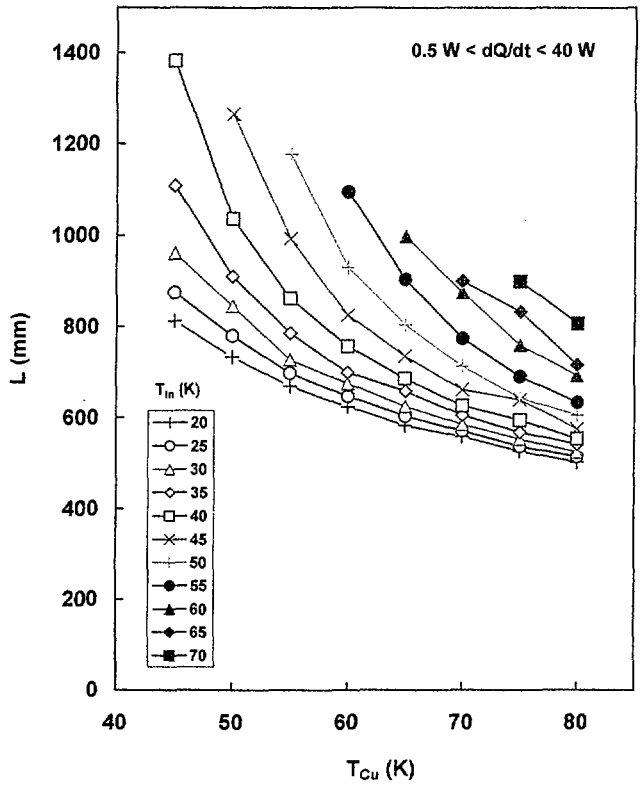

Fig. 13. Optimum length of the heat exchanger versus the temperature at the cold end for helium inlet temperatures between 20 and 70 K.

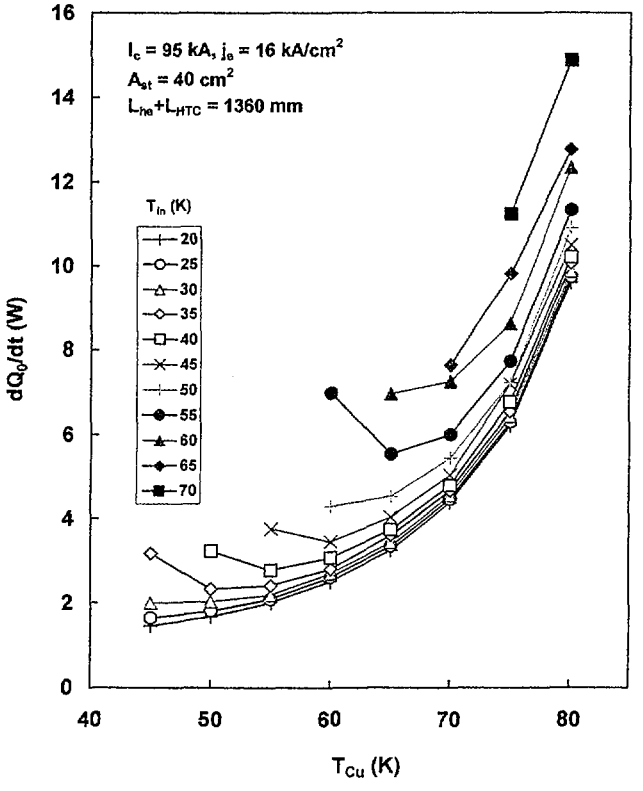

Fig. 14. Heat load at 4.5 K versus the temperature at the cold end of the heat exchanger. The length of the binary current lead is 1360 mm, the design value of I_c is 95 kA and the cross-section of the stainless steel support of the HTS part is 40 cm^2.

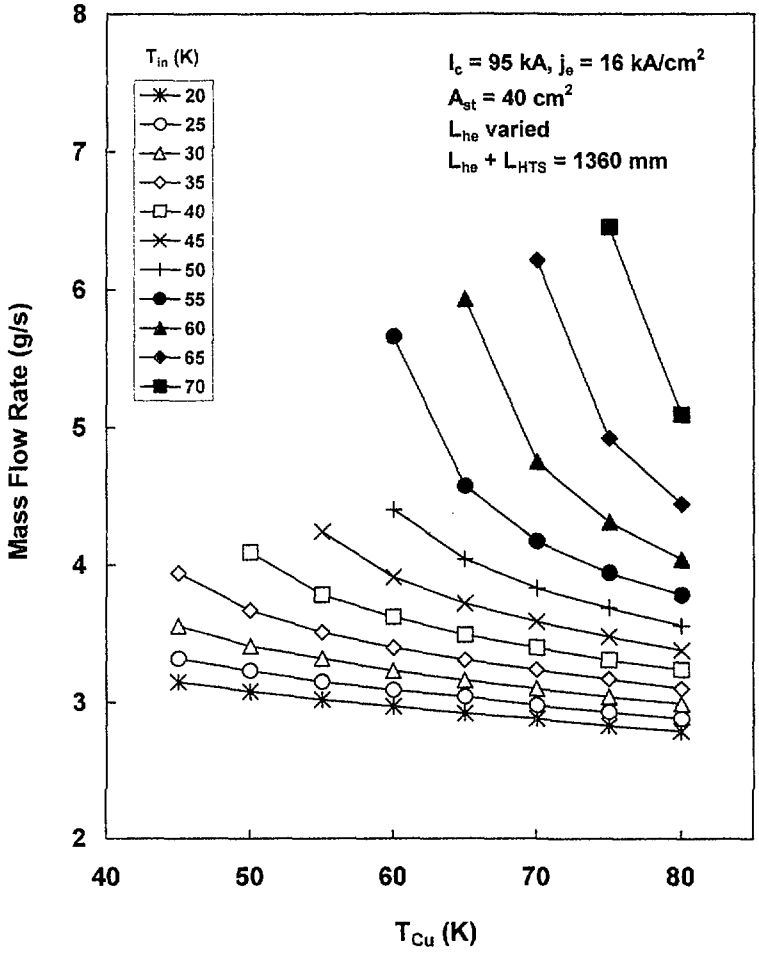

Fig 15. Mass flow rate required to cool the heat exchanger part versus the copper temperature at the cold end.

Fig. 16 shows the electrical input power required by an ideal refrigerator to cool the current lead as a function of the helium inlet temperature for copper temperatures at the cold end of the heat exchanger in the 45 – 80 K range. A minimum of the required refrigerator input power results for each of the cold end conductor temperatures when the difference of the coolant and the conductor temperature at the cold end is between 15 and 20 K. The lowest refrigerator input power results for helium inlet temperatures of 55 - 60 K and conductor temperatures of 75 – 80 K. However, the required refrigerator input power is enhanced by less than 10 % when the temperatures of the conductor and the helium at the cold end are reduced to values of 65 and 45 K, respectively.

Fig. 17 shows the electrical input power required by a real refrigerator to cool the current lead as a function of the helium inlet temperature for copper temperatures at the cold end of the heat exchanger in the 45 – 80 K range. Except the much larger required refrigerator input power the behaviour with respect to the optimum conductor and helium temperatures at the cold end is very similar to that found for ideal cooling cycles. The smallest refrigerator power is required for conductor temperatures between 70 and 80 K. The optimum difference of the conductor and the coolant temperature at the cold end is slightly reduced to values in the 10 - 15 K range. Thus, the optimum helium inlet temperature is between 55 and 60 K. For a conductor temperature of 60 K and a helium inlet temperature of 50 K the required refrigerator input power is 18 % higher than the minimum value for T_i = 75 K and T_{in} = 60 K.

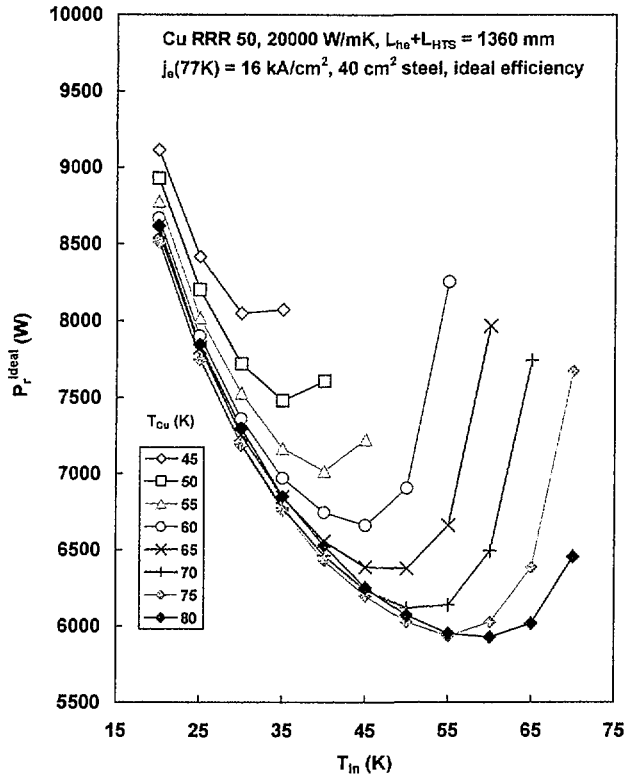

Fig. 16. Required refrigerator input power to cool the whole binary current lead versus the helium inlet temperature for copper temperatures in the 45 – 80 K range at the cold end. The data are for ideal cooling cycles.

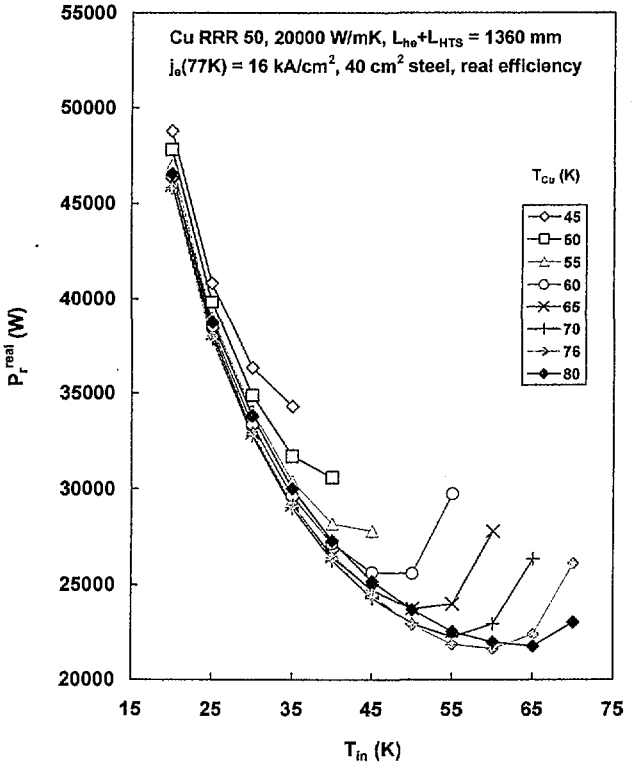

Fig. 17. Required refrigerator input power to cool the whole binary current lead versus the helium inlet temperature for copper temperatures in the 45 – 80 K range at the cold end. The data are for real cooling cycles.

Binary current lead of 1360 mm length (Cu *RRR* = 50, *hP* = 20000 W/mK, j_e(77 K, 0) = 12 kA/cm^2)

Fig. 18 shows the heat load at 4.5 K which results for a design value of the critical current of 95 kA and an engineering critical current density of 12 kA/cm^2 at 77 K and zero applied field. The cross-section of the stainless steel support of the HTS part of the current lead is 40 cm^2. Furthermore, a constant length of the binary current lead of 1360 mm has been selected for the calculations. The warm and cold end connections as well as the connection between the HTS and the heat exchanger have been taken not into consideration. As long as the heat exchanger part is sufficiently short the heat load at 4.5 K decreases with decreasing temperature at the warm end of the HTS part. Reduced helium inlet temperatures lead to decreasing heat loads at 4.5 K.

Fig. 19 shows the electrical input power required by an ideal refrigerator to cool the current lead as a function of the helium inlet temperature for copper temperatures at the cold end of the heat exchanger in the 45 – 80 K range. The minimum of the required refrigerator input power is reached for a helium inlet temperature of 55 K and a conductor temperature of 75 K at the cold end of the heat exchanger. However, the required refrigerator input power is only slighty enhanced when the conductor and the helium temperature at the cold end of the heat exchanger are reduced to 60 and 50 K, respectively.

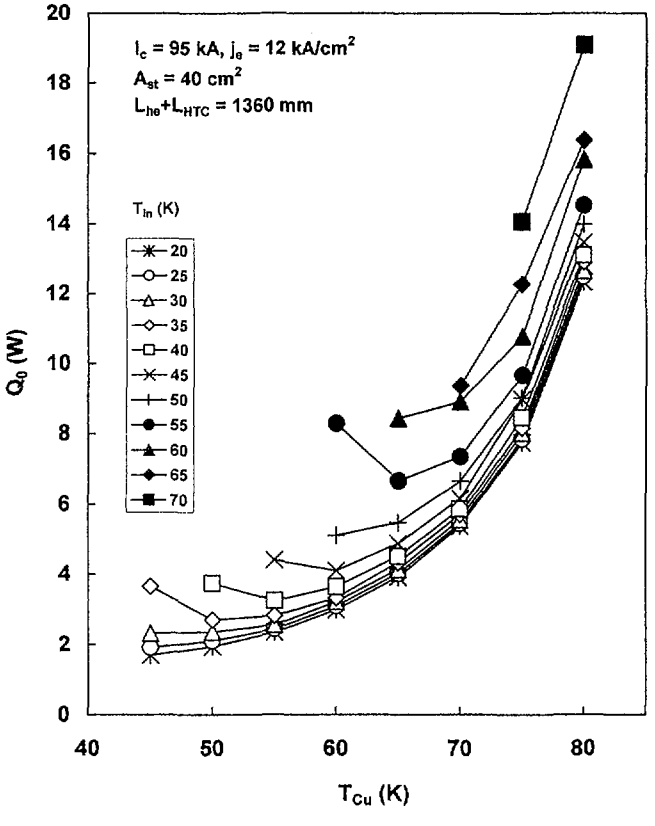

Fig. 18. Heat load at 4.5 K versus the conductor temperature at the cold end of the heat exchanger. The helium inlet temperature has been varied between 20 and 70 K. The total length of the heat exchanger and the HTS part is 1360 mm. The cross-section of the stainless steel support of the HTS part is 40 cm^2.

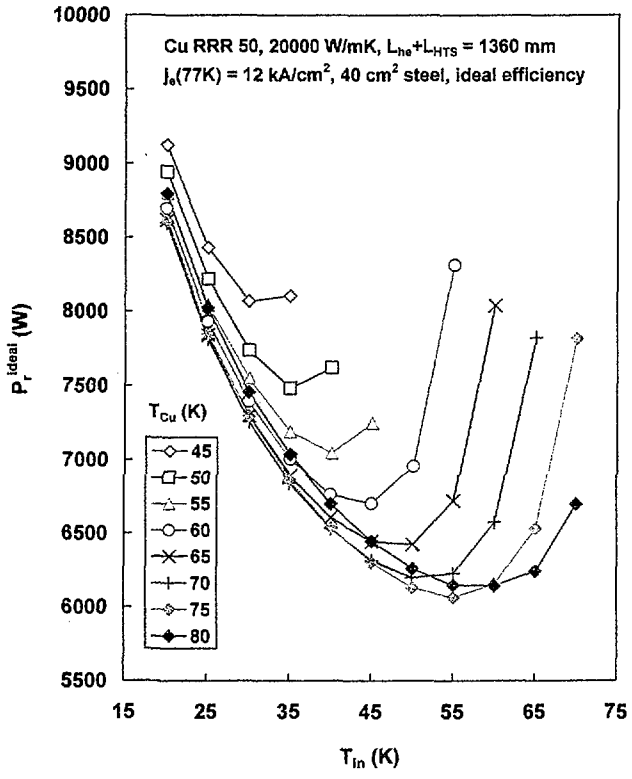

Fig. 19. Required refrigerator input power to cool the whole binary current lead versus the helium inlet temperature for copper temperatures in the 45 – 80 K range at the cold end. The data are for ideal cooling cycles.

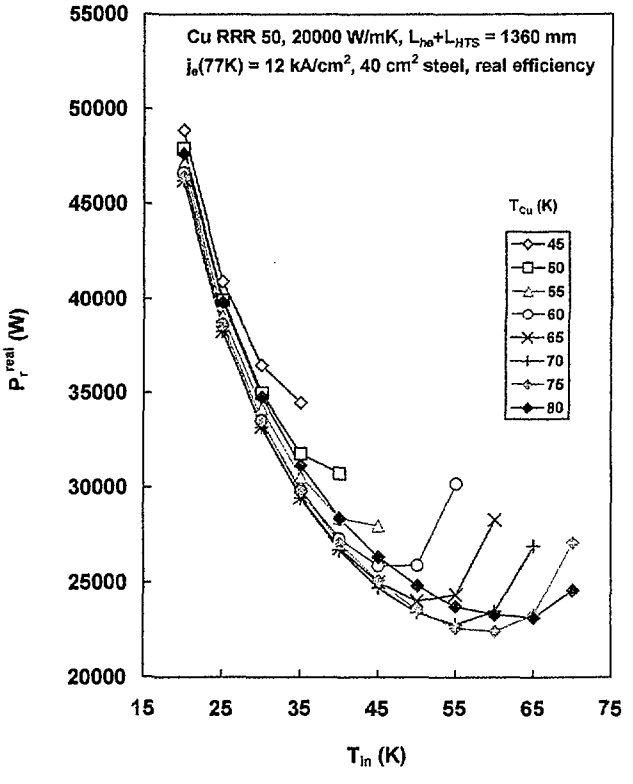

Fig. 20. Required refrigerator input power to cool the whole binary current lead versus the helium inlet temperature for copper temperatures in the 45 – 80 K range at the cold end. The data are for real cooling cycles.

Fig. 20 shows the electrical input power required by a real refrigerator to cool the current lead as a function of the helium inlet temperature for copper temperatures at the cold end of the heat exchanger in the 45 – 80 K range. The minimum of the required refrigerator input power is reached for a helium inlet temperature of 60 K and a conductor temperature of 75 K. But even for a conductor temperature of 60 K and a helium inlet temperature of 45 K the required refrigerator input power is only slightly enhanced.

Binary current lead of 1360 mm length (Cu *RRR* = 50, *hP* = 20000 W/mK, j_e(77 K, 0) = 8 kA/cm^2)

Fig. 21 shows the heat load at 4.5 K which results for a design value of the critical current of 95 kA and an engineering critical current density of 8 kA/cm^2 at 77 K and zero applied field. The cross-section of the stainless steel support of the HTS part of the current lead is 40 cm^2. Again a constant length of the binary current lead of 1360 mm has been selected for the model calculations. The warm and cold end connections as well as the connection between the HTS and the heat exchanger have been taken not into consideration. As long as the heat exchanger part is sufficiently short the heat load at 4.5 K decreases with decreasing temperature at the warm end of the HTS part. Reduced helium inlet temperatures lead to decreasing heat loads at 4.5 K. Fig. 22 shows the electrical input power required by an ideal refrigerator to cool the current lead as a function of the helium inlet temperature for copper temperatures at the cold end of the heat exchanger in the 45 – 80 K range.

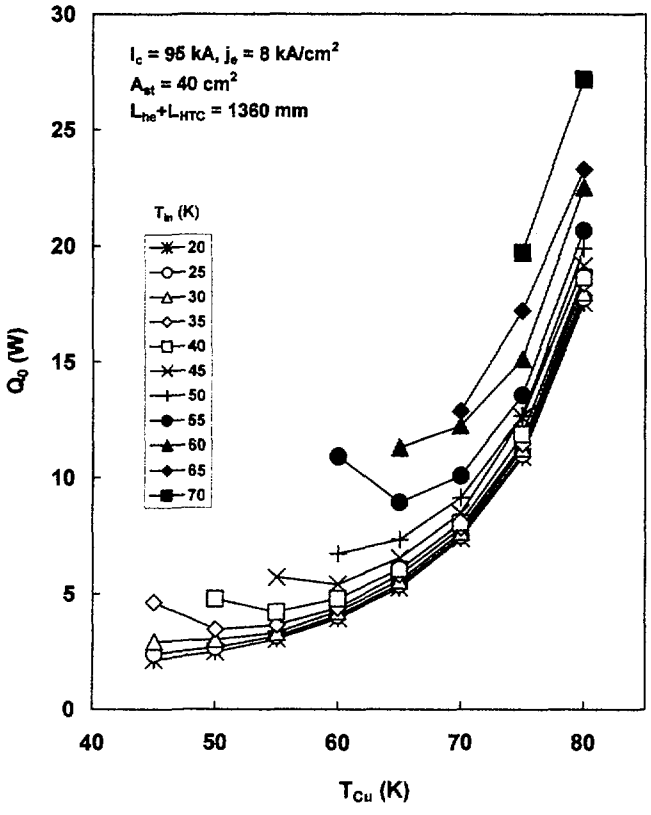

Fig. 21. Heat load at 4.5 K versus the conductor temperature at the cold end of the heat exchanger. The total length of the heat exchanger and the HTS part is 1360 mm. The cross-section of the stainless steel support of the HTS part is 40 cm^2.

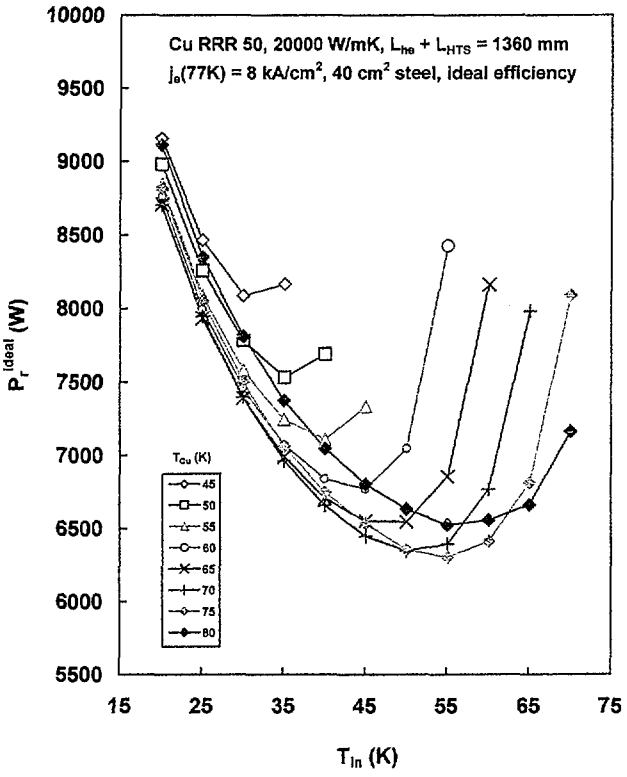

Fig. 22. Required refrigerator input power to cool the whole binary current lead versus the helium inlet temperature for copper temperatures in the 45 – 80 K range at the cold end. The data are for ideal cooling cycles.

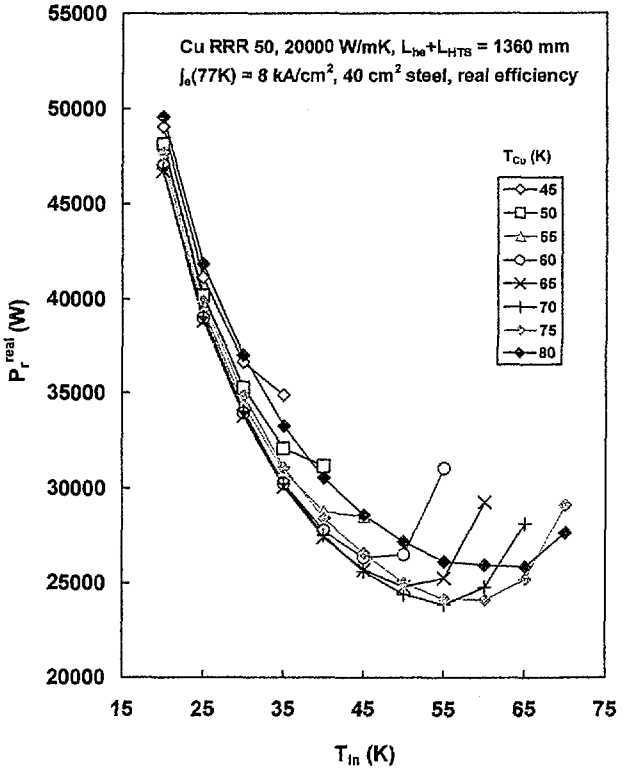

Fig. 23. Required refrigerator input power to cool the whole binary current lead versus the helium inlet temperature for copper temperatures in the 45 – 80 K range at the cold end. The data are for real cooling cycles.

The minimum of the required refrigerator input power is reached for a helium inlet temperature of 55 K and a conductor temperature of 75 K at the cold end of the heat exchanger. However, the required refrigerator input power is only slighty enhanced when the conductor and the helium temperature at the cold end of the heat exchanger are reduced to 60 and 45 K, respectively.

Fig. 23 shows the electrical input power required by a real refrigerator to cool the current lead as a function of the helium inlet temperature for copper temperatures at the cold end of the heat exchanger in the 45 – 80 K range. The minimum of the required refrigerator input power is reached for a helium inlet temperature of 55 K and a conductor temperature of 70 K. But even for a conductor temperature of 60 K and a helium inlet temperature of 45 K the required refrigerator input power is only slightly enhanced.

Binary current lead of 1360 mm length with an enhanced stainless steel cross-section of 100 cm^2 (Cu *RRR* = 50, hP = 20000 W/mK, j_c(77 K, 0) = 8 kA/cm^2)

Fig. 24 shows the heat load at 4.5 K as a function of the copper temperature at the cold end of the heat exchanger for a stainless steel cross-section of 100 cm^2. Again a total length of the heat exchanger and the HTS part of 1360 mm has been selected for the model calculations. As long as the heat exchanger part is sufficiently short the heat load at 4.5 K decreases with decreasing temperature at the warm end of the HTS part. Moreover, reduced helium inlet temperatures are advantageous.

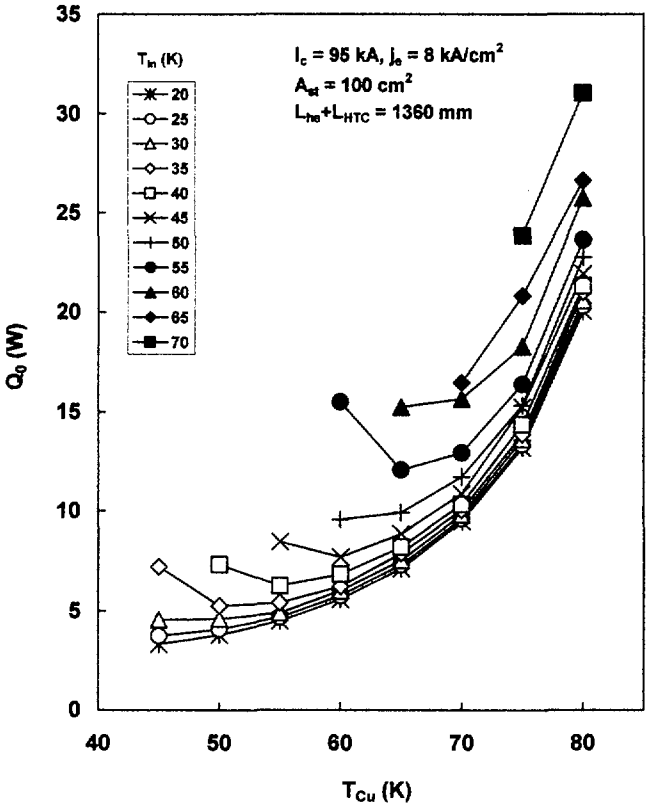

Fig. 24. Heat load at 4.5 K versus the conductor temperature at the cold end of the heat exchanger. The total length of the heat exchanger and the HTS part is 1360 mm. The cross-section of the stainless steel support of the HTS part is 100 cm^2.

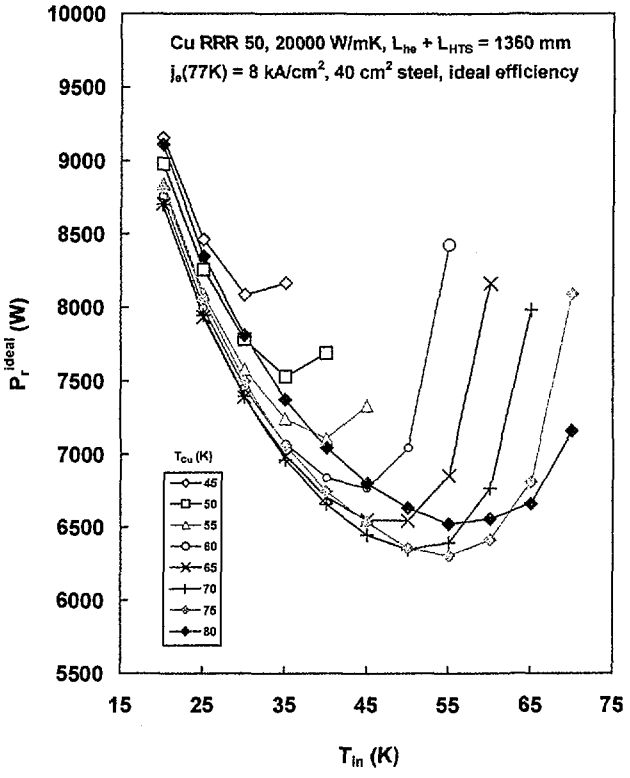

Fig. 25. Required refrigerator input power to cool the whole binary current lead versus the helium inlet temperature for copper temperatures in the 45 – 80 K range at the cold end. The data are for ideal cooling cycles.

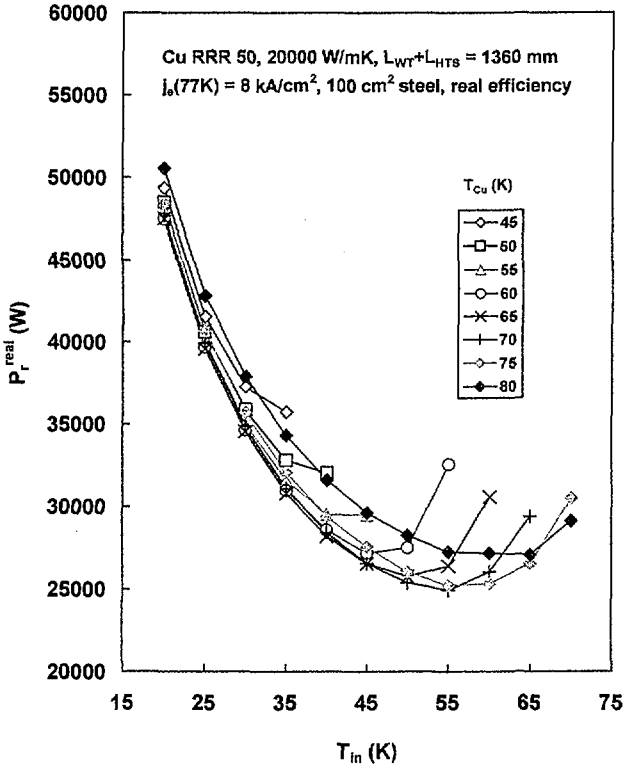

Fig. 26. Required refrigerator input power to cool the whole binary current lead versus the helium inlet temperature for copper temperatures in the 45 – 80 K range at the cold end. The data are for real cooling cycles.

Figures 25 and 26 show the refrigerator input power required to cool the whole current lead for ideal and real cooling cycles, respectively. The minimum refrigerator input power required to cool the whole current lead is reached for T_{in} = 55 K and T_{Cu} = 75 K assuming an ideal cooling cycle. The corresponding temperatures for a real cooling cycle are T_{in} = 55 K and T_{Cu} = 70 K.

Heat exchanger length, mass flow rate and required refrigerator input power

In the previous model calculations the length of the heat exchanger part has been varied in such a way that the optimum mass flow rate for a current of 68 kA can be reached. For the optimum mass flow rate the heat flux at the warm end of the heat exchanger part is zero. To obtain a total length of the heat exchanger and the HTS part of 1360 mm, the length of the HTS part has been varied. Mass flow rates slightly higher than the optimum value can be used to reduce the length of the heat exchanger part considerably. Fig. 27 shows the length of the heat exchanger as a function of the mass flow rate for cold end helium and conductor temperatures of 55 and 70 K, respectively. The length of the HTS part has been selected in such a way that the total length of the HTS part and the heat exchanger is 1360 mm. Enhanced mass flow rates lead to a longer HTS part, and hence a reduced heat load at 4.5 K. Taking into consideration the heat load at the cold end of the HTS part the minimum of the refrigerator power required to cool the whole current lead is reached for a mass flow rate which is 0.5 % higher than the optimum value.

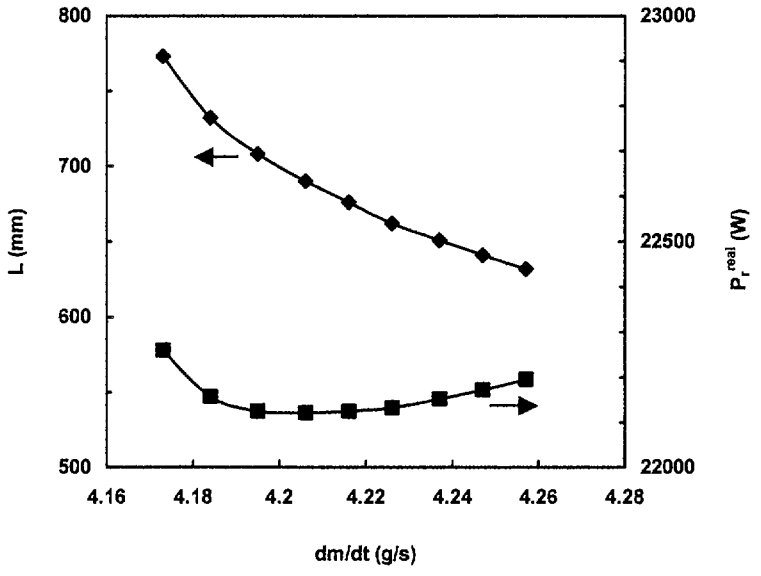

Fig. 27. Length of the heat exchanger (blue diamonds) as a function of the mass flow rate. The refrigerator input power (pink squares) required to cool the whole current lead reaches a minimum for a mass flow rate which is 0.5 % higher than the optimum value.

Binary current lead with an HTS part of 600 mm length and variable total length (Cu *RRR* = 50, hP = 20000 W/mK, j_e(77 K, 0) = 16 kA/cm^2)

In the following simulations a length of 600 mm has been selected for the HTS part, while the length of the heat exchanger is optimised regarding the mass flow rate. Thus, the total length of the current lead is varying. The cross-section of the stainless steel support in the HTS part of the current lead is 40 cm^2. Fig. 28 shows the resulting heat load at the cold end of the HTS part.

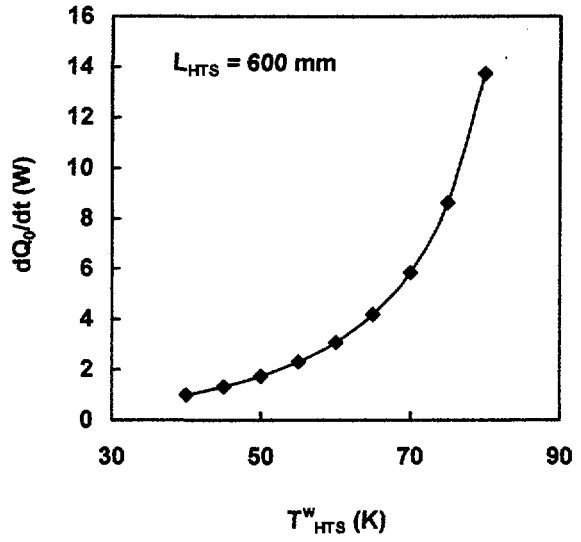

Fig. 28. Heat load at 4.5 K as a function of the temperature at the warm end of the superconductor. The data are based on a stainless steel cross-section of 40 cm^2 and a length of the HTS part of 600 mm.

Fig. 29 shows the refrigerator input power required to cool the current lead. The data shown in Fig. 29 are based on ideal cooling cycles. The minimum of the required refrigerator input power is reached for a helium inlet temperature of 55 K and and a conductor temperature of 75 K. The power consumed to cool the current lead is only slightly enhanced when T_{in} and T_{Cu} are reduced to values of 50 and 65 K, respectively.

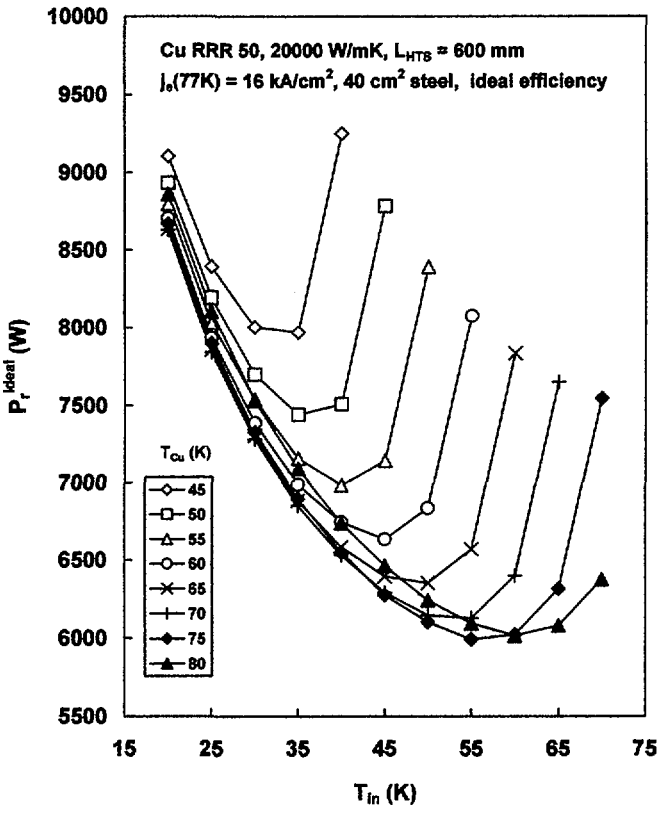

Fig. 29. Refrigerator input power required to cool the whole current lead as a function of the helium inlet temperature for copper temperatures between 45 and 80 K at the cold end of the heat exchanger. The data are based on an ideal cooling cycle.

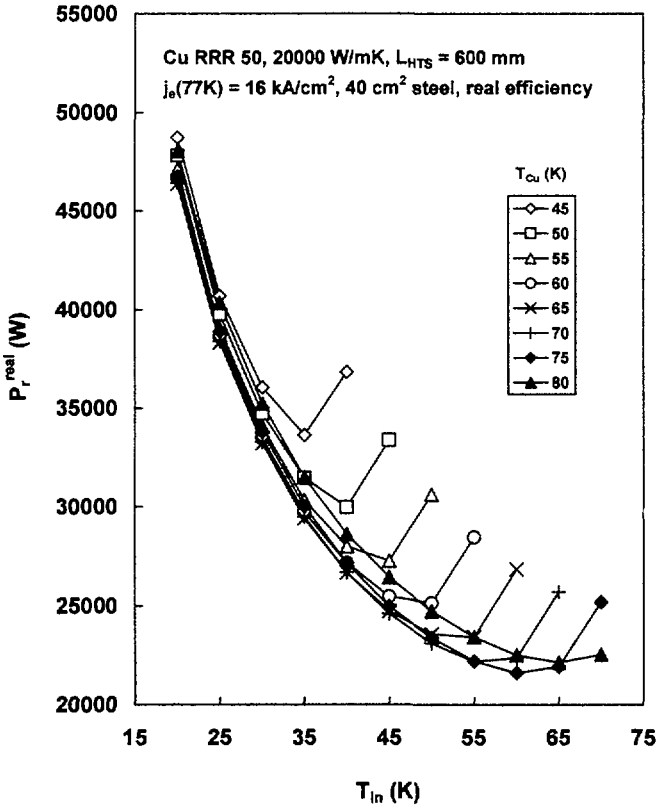

Fig. 30. Refrigerator input power required to cool the whole current lead as a function of the helium inlet temperature for copper temperatures between 45 and 80 K at the cold end of the heat exchanger. The data are based on a real cooling cycle.

Fig. 30 shows the refrigerator input power required to cool the current lead as a function of the helium inlet temperature for different copper temperatures at the cold end of the heat exchanger. The values shown in Fig. 30 have been obtained assuming a real refrigerator. The optimum values of T_{in} and T_{Cu} with respect to the required refrigerator input power are 60 and 75 K, respectively. The required refrigerator input power for slightly reduced helium and conductor temperatures at the cold end of the heat exchanger is not significantly enhanced.

Effect of the cooling parameter *hP*

Fig. 31 shows the required refrigerator input power as a function of the helium inlet temperature for copper temperatures at the cold end of the heat exchanger in the 45 – 80 K range. The results shown in Fig. 31 are for ideal reversible cooling cycles. The residual resistivity ratio of the copper used in the simulations is 30. The length of the HTS part is 600 mm, while the length of the heat exchanger part is varied to reach the optimum mass flow rate. The cross-section of the superconductor is selected in such a way that the critical current based on a j_e value of 16 kA/cm^2 at 77 K and B = 0 reaches 95 kA at the warm end. The cross-section of the stainless steel support is 40 cm^2. The data shown on the left are for a cooling parameter *hP* of 40000 W/mK, while those on the right are for a *hP* value of 20000 W/mK. Fig. 31 indicates that the position of the minimum of the required refrigerator input power needed to cool the whole current lead is practically independent of the cooling parameter *hP*.

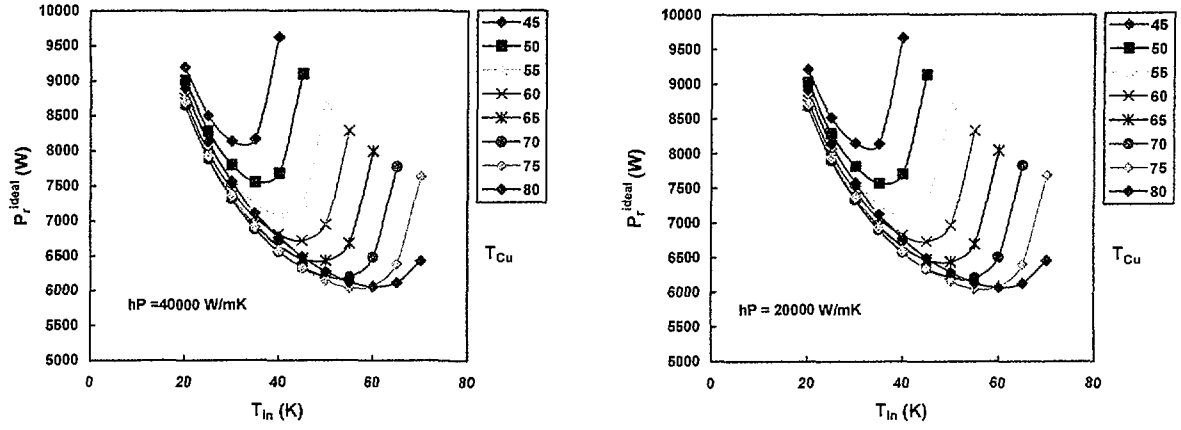

Fig. 31. Refrigerator input power required to cool the whole current lead as a function of the helium inlet temperature for selected values of the copper temperature at the cold end of the heat exchanger. The data on the left are for hP = 40000 W/mK and those on the right for hP = 20000 W/mK.

Effect of the residual resistivity ratio of the copper

Next, the effect of the residual resistivity ratio of the copper on the refrigerator input power required to cool the whole current lead has been considered. The simulations are based on ideal reversible cooling cycles, a design value of the critical current of 95 kA (j_e(77 K, 0) = 16 kA/cm^2), a stainless steel cross-section of 40 cm^2, a constant length of the HTS part of 600 mm and a cooling parameter of 20000 W/mK. The length of the heat exchanger is varied to reach the optimum value of the mass flow rate. Fig. 32 shows the input power of the refrigerator needed to cool the current lead as a function of the helium inlet temperature for selected copper temperatures at the cold end of the heat exchanger.

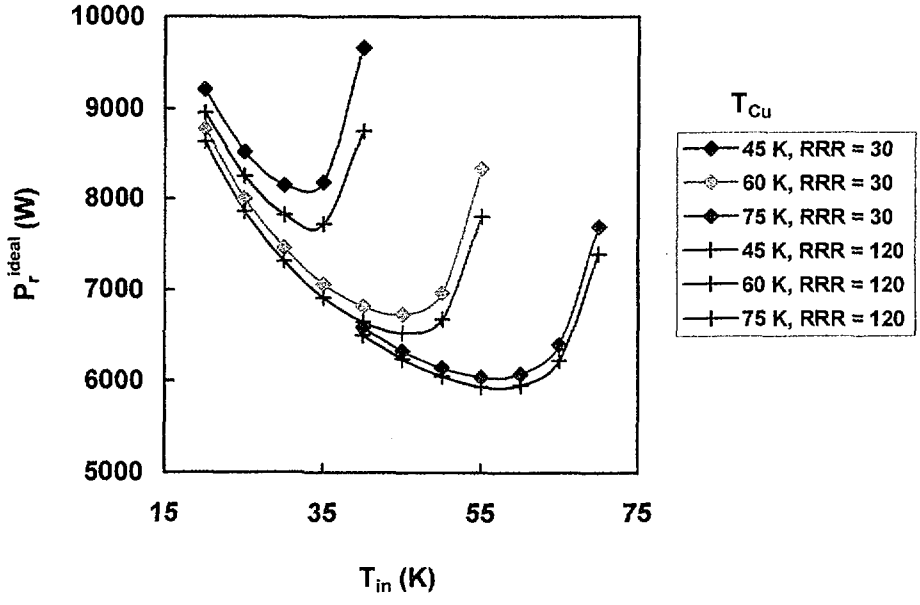

Fig. 32. Input power required to cool the whole current lead versus the helium inlet temperature for copper with residual resistivity ratios of 30 and 120.

The use of copper with a higher residual resistivity ratio provides a slightly reduced value of the required refrigerator input power. On the other hand, the position of the minimum regarding the conductor temperature at the cold end of the heat exchanger is not significantly changed. The length of the heat exchanger for selected values of T_{in} and T_{Cu} is given in Table 6. The length of the heat exchanger has to be considerably enhanced for the higher value of the residual resistivity ratio.

Table 6. Length of the heat exchanger for *RRR* values of 30 and 120 and selected operating conditions.

Operating conditions	*RRR* = 30	*RRR* = 120
T_{in} = 35 K T_{Cu} = 45 K	dm/dt = 4.056 g/s L = 1124 mm	dm/dt = 3.825 g/s L = 1277 mm
T_{in} = 55 K T_{Cu} = 75 K	dm/dt = 3.977 g/s L = 698 mm	dm/dt = 3.900 g/s L = 741 mm

Effect of the engineering critical current density

The heat load at 4.5 K depends on the temperature at the warm end of the HTS and the cross-sections of superconductor and stainless steel support. The superconductor cross-section is determined by the desired critical current at the warm end and the engineering critical current density. The ratio of $j_e(B,T)/j_e(77\ K, 0)$ is expected to be independent of the value of $j_e(77\ K, 0)$ of the AgAu/Bi-2223 tape. Fig. 33 shows the input power required by a real refrigerator to cool the current lead as a function of the temperature of the copper at the cold end of the heat exchanger for a helium inlet temperature of 20 K.

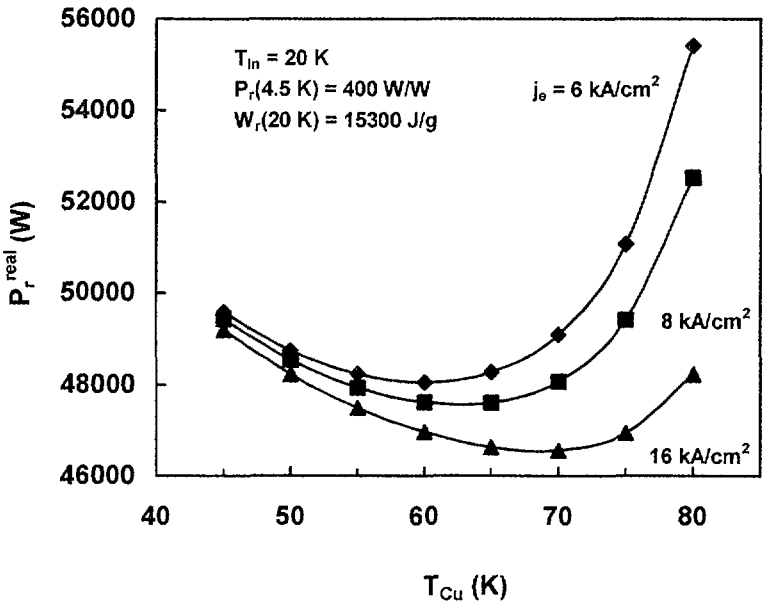

Fig. 33. Refrigerator input power required to cool current leads constructed of AgAu/Bi-2223 tapes with $j_e(77\ K, 0)$ values of 6, 8 and 16 kA/cm^2. Due to the enhanced heat load caused by a larger superconductor cross-section the required refrigerator input power increases with decreasing j_e. The optimum conductor temperature at the cold end of the heat exchanger is shifted to lower values for reduced critical current densities.

A residual resistivity ratio of 30, a stainless steel cross-section of 40 cm^2 and a cooling parameter of 40000 W/mK have been used in the simulations. A reduction of the engineering critical current density at 77 K and zero applied field from 16 to 6 kA/cm^2 enlarges the heat load at 4.5 K especially for the highest copper temperatures at the cold end of the heat exchanger. This behaviour reflects the larger contribution of the heat load at 4.5 K to the required refrigerator input power for higher temperatures at the warm end of the superconductor. In addition to the absolutely enhanced input power needed by the refrigerator, the optimum conductor temperature is shifted from ≈70 K to ≈60 K.

Effect of the cross-section of the stainless steel support

Next, the effect of the cross-section of the stainless steel support in the HTS part of the current lead on the required refrigerator input power is considered. Simulations have been performed for stainless steel cross-sections of 40, 80 and 120 cm^2, an engineering critical current density of the AgAu/Bi-2223 tapes of 16 kA/cm^2 at 77 K and $B = 0$, a residual resistivity ratio of 30 and a cooling parameter of 40000 W/mK. Fig. 34 shows the required refrigerator input power as a function of the copper temperature at the cold end of the heat exchanger for a helium inlet temperature of 20 K. The required refrigerator input power is enhanced for a larger stainless steel cross-section, which is responsible for an enlarged heat load at 4.5 K.

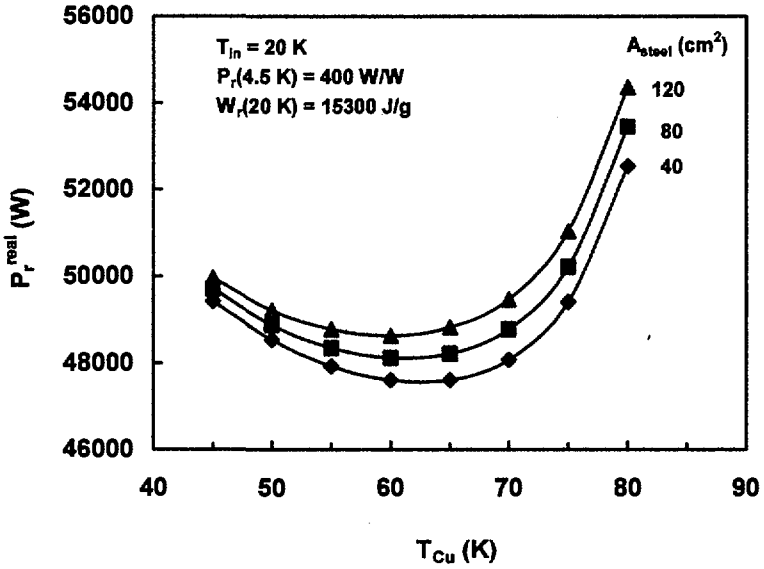

Fig. 34. Refrigerator input power required to cool current leads with stainless steel cross-sections of 40, 80 and 120 cm^2 versus the conductor temperature at the cold end of the heat exchanger. For larger stainless steel cross-sections the optimum cold end conductor temperature is lowered.

Variation of the refrigerator efficiency

The optimum conductor temperature at the cold end of the heat exchanger depends also on the efficiency of the cooling cycles. Fig. 35 shows the required refrigerator input power as a function of the copper temperature at the cold end of the heat exchanger for a helium inlet temperature of 20 K. When the efficiency of the 20 K cooling cycle is enhanced while that for the 4.5 K heat load is unchanged, the optimum conductor temperature is shifted to lower values.

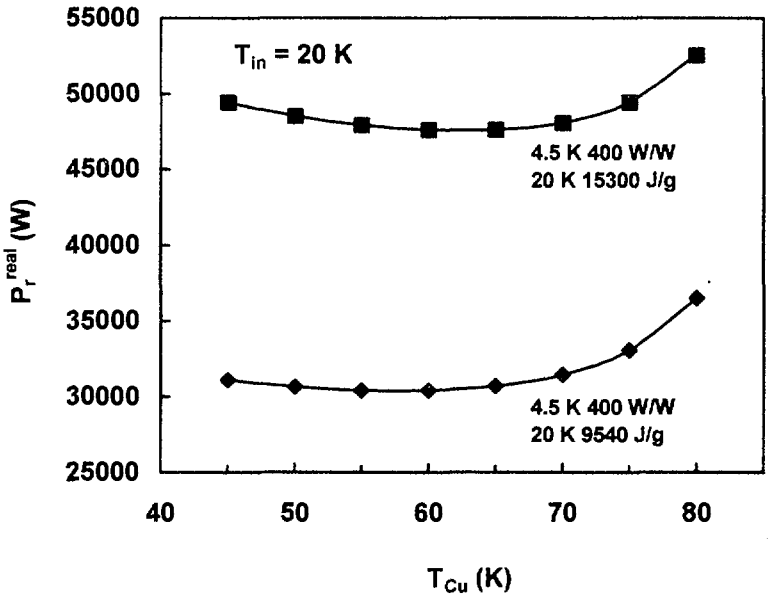

Fig. 35. Refrigerator input power required to cool the current lead versus the copper temperature at the cold end of the heat exchanger for two different efficiencies of the 20 K cooling loop. An enhanced efficiency of the 20 K loop favours lower temperatures of the copper at the cold end of the heat exchanger.

Conduction-cooled connection of HTS and heat exchanger part

So far, the connection between the HTS and the heat exchanger part has been neglected. Because of the small changes of the temperature within the connection the variation of the resistivity and the thermal conductivity can be neglected. The temperature profile is therefore given by $T(x) = -(a/2)x^2 + bx + c$, where $a = (\rho/\lambda)j^2$. The integration constants can be determined from the temperature and the heat flux at the lower end of the connection which are equal to the warm end temperature of the HTS and the heat flux at 4.5 K. Fig. 36 shows the temperature profile and the heat flux in the connection which would result for copper with a residual resistivity ratio of 50, a cross-section of 200 cm^2 and a length of 6 cm. The heat flux at 4.5 K is 4.2 W for a superconductor temperature of 65 K at the warm end. The temperature in the connection reaches a maximum close to the connection to the HTS part. The heat generated in the connection flows mainly to the heat exchanger, and hence an enhanced mass flow rate is required to cool the heat exchanger part.

Fig. 37 shows the input power of an ideal refrigerator required to cool a binary current lead with and without a conduction-cooled connection between the HTS and the heat exchanger as a function of the warm end HTS temperature for a helium inlet temperature of 50 K. Taking into consideration the connection the refrigerator input power required to cool the whole current lead is enhanced. However, the optimum temperature at the warm end of the HTS is practically unchanged.

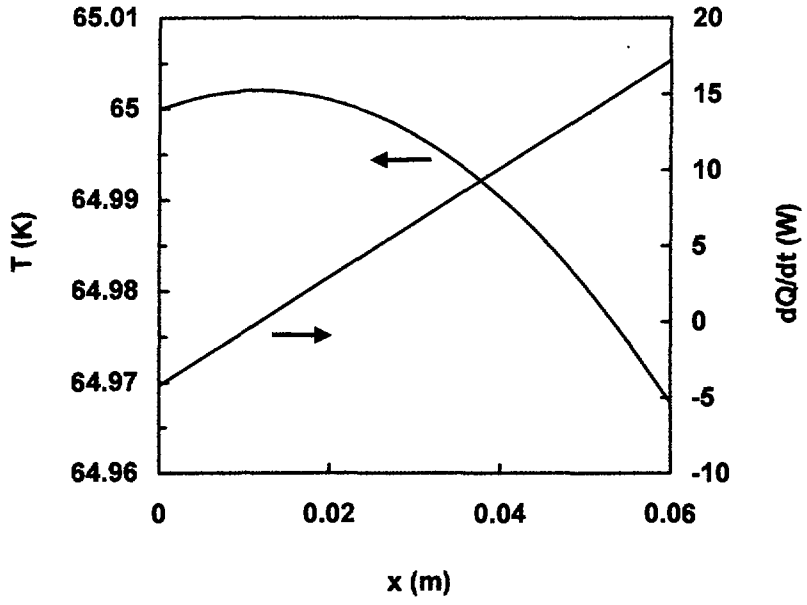

Fig. 36. Temperature profile and heat flux in the conduction-cooled connection between the HTS and the heat exchanger.

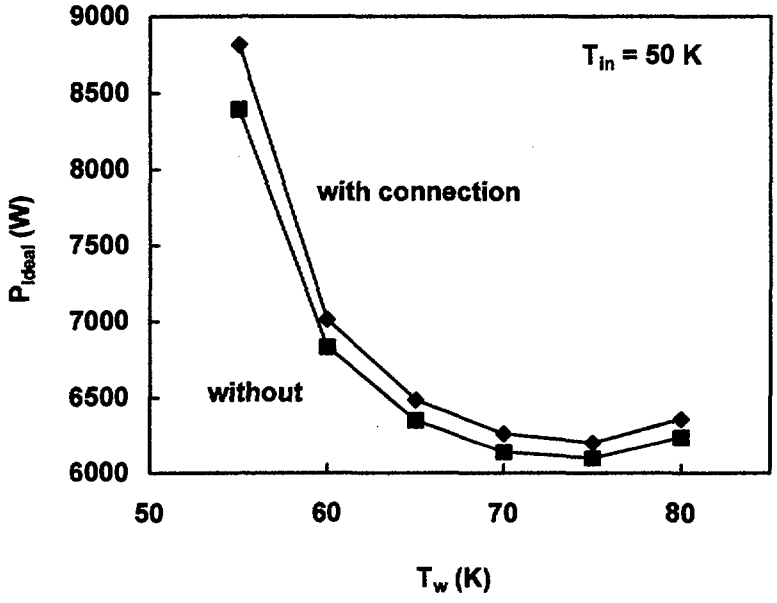

Fig. 37. Refrigerator input power required to cool a binary current lead with and without a conduction-cooled connection between the HTS and the heat exchanger part. The heat exchanger is actively cooled by helium gas of 50 K inlet temperature. The optimum conductor temperature at the cold end of the heat exchanger is in both cases ≈75 K.

Conclusions

The thermal behaviour of binary 70 kA HTS current leads has been simulated numerically. The optimum temperature of the helium and the conductor at the cold end of the heat exchanger have been found to depend on the assumed refrigerator efficiency, the engineering critical current density of the AgAu/Bi-2223 tapes at the envisaged temperature at the warm end of the superconductor and the cross-section of the stainless steel support.

Reduced engineering critical current densities as well as enlarged stainless steel cross-sections lead to a larger heat load at 4.5 K. As a consequence, the optimum temperature at the warm end of the HTS is shifted in both cases to lower values.

When the efficiency of the intermediate temperature cooling cycle providing helium gas of the temperature T_{in} is enhanced with respect to the efficiency of the 4.5 K cooling cycle the optimum temperature at the warm end of the HTS is shifted to lower values.

Considering ideal cooling cycles the optimum intermediate conductor temperature (warm end of HTS, cold end of heat exchanger) is between 75 and 80 K for a stainless steel cross-section of 40 cm^2 and a total length of 1360 mm (HTS and heat exchanger without connections). The optimum difference of the conductor and the helium temperature at the cold end of the heat exchanger is approximately 20 K. However, even for a conductor temperature of 65 K and a helium inlet temperature of 45 K the required refrigerator input power needed to cool the current lead is only slightly enhanced.

In the case of real cooling cycles the optimum intermediate conductor temperature is between 70 and 80 K for a stainless steel cross-section of 40 cm^2 and a total length of 1360 mm. The optimum difference of the conductor and helium temperature at the cold end of the heat exchanger is approximately 15 K.

The safety requirements in the case of loss of flow favour a design with small values of j_{op}/j_e, a low temperature and an enhanced stainless steel cross-section at the warm end of the HTS. Reduced operating current densities and a lower warm end temperature provide an enhanced temperature margin. A large stainless steel cross-section increases the heat capacity of the HTS part of the current lead. Both measures would considerably prolong the time available to discharge the toroidal field coils in the case of loss of flow.

Acknowledgment

This work was performed in the frame of the Task EFDA 01/598 within the European Fusion Technology Programme of the Centre de Recherches en Physique des Plasmas, Villigen, Switzerland and the Forschungszentrum Karlsruhe, Germany.

References

1. R. Heller, M. Tasca, P. Erismann, A.M. Fuchs, M. Vogel, IEEE Trans. on Appl. Supercond. **10,** 1470 (2000)

2. M. Tasca, "Entwicklung und Verifizierung einer modularen Hochstromzuführung unter Verwendung von Hochtemperatursupraleitern," Dissertation, Wissenschaftliche Berichte FZKA 6608 (2001)

3. M.N. Wilson, *Superconducting Magnets*, Clarendon Press, Oxford, UK (1983)

4. J.L. Wu, J.T. Dederer, P.W. Eckels, S.K. Singh et al., IEEE Trans. Magn. **MAG-27**, 1861 (1991)

5. R. Wesche, A.M. Fuchs, Cryogenics **34**, 145 (1994)

6. A. Ballarino, "Current leads for the LHC magnet system", paper presented at the MT 17, Geneva, Switzerland, September 24-28, 2001

7. R. Heller, G. Friesinger, A.M. Fuchs, R. Wesche, "Development of high temperature superconductor current leads for 70 kA", paper presented at the MT 17, Geneva, Switzerland, September 24-28, 2001